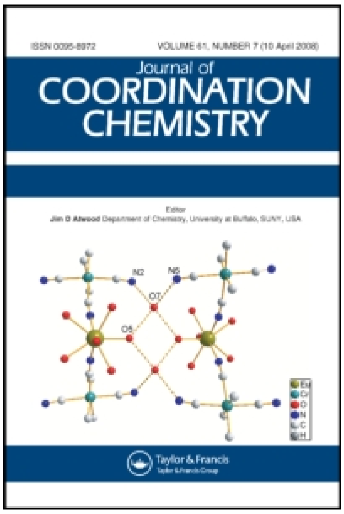

Journal of Coordination Chemistry

Publication details, including instructions for authors and subscription information:
http://www.informaworld.com/smpp/title~content=t713455674

Synthesis, crystal structure, spectroscopy, and magnetism of a mixed valence Co(III)-Co(II)-Co(III) complex stabilized by *N*-(2-hydroxybenzyl)salicylaldimine

Chun Yang[ab]; Qing-Lun Wang[a]; Guo-Tao Tang[a]; Chao Wang[a]; Shi-Ping Yan[a]; Dai-Zheng Liao[a]
[a] Department of Chemistry, Nankai University, Tianjin 300071, P.R. China [b] School of Chemical Engineering and Technology, Hebei University of Technology, Tianjin 300130, P.R. China

First published on: 19 January 2010

To cite this Article Yang, Chun , Wang, Qing-Lun , Tang, Guo-Tao , Wang, Chao , Yan, Shi-Ping and Liao, Dai-Zheng(2010) 'Synthesis, crystal structure, spectroscopy, and magnetism of a mixed valence Co(III)-Co(II)-Co(III) complex stabilized by *N*-(2-hydroxybenzyl)salicylaldimine', Journal of Coordination Chemistry, 63: 3, 505 — 514, First published on: 19 January 2010 (iFirst)

To link to this Article: DOI: 10.1080/00958970903509277

URL: http://dx.doi.org/10.1080/00958970903509277

Journal of Coordination Chemistry
Vol. 63, No. 3, 10 February 2010, 505–514

Synthesis, crystal structure, spectroscopy, and magnetism of a mixed valence Co(III)–Co(II)–Co(III) complex stabilized by *N*-(2-hydroxybenzyl)salicylaldimine

CHUN YANG†‡, QING-LUN WANG*†, GUO-TAO TANG†, CHAO WANG†, SHI-PING YAN† and DAI-ZHENG LIAO†

†Department of Chemistry, Nankai University, Tianjin 300071, P.R. China
‡School of Chemical Engineering and Technology, Hebei University of Technology, Tianjin 300130, P.R. China

(*Received 20 July 2009; in final form 2 September 2009*)

Reaction of $Co(OAc)_2 \cdot 4H_2O$ with *N*-(2-hydroxybenzyl)salicylaldimine (H_2L_a) in dimethylformamide (DMF)–H_2O yields a linear trinuclear mixed valence complex $[Co^{III}(\mu\text{-}L_a)(\mu\text{-}L_b)(\mu\text{-}OAc)]_2Co^{II} \cdot 2DMF$ (**1**). Here, HL_b is salicylaldimine, which is afforded by an *in situ* transformation of H_2L_a via cleavage of the C–N bond. Complex **1** has been characterized by X-ray crystallography as well as elemental analysis, UV-Vis, and IR spectroscopy. The cathodic and anodic responses of **1** in DMF appeared at −1.46 V ($Co^{III} \rightarrow Co^{II}$, quasi-irreversible) and +0.99 V ($Co^{II} \rightarrow Co^{III}$, irreversible) *versus* saturated calomel electrode, respectively. The magnetic behavior of **1** has been analyzed by the one-ion approximation with spin–orbit coupling in O_h symmetry giving $\lambda = -121\,cm^{-1}$.

Keywords: Mixed valence; Trinuclear cobalt complex; Crystal structure; Magnetic properties

1. Introduction

Multinuclear complexes of transition metal ions attract considerable attention for molecular magnetism [1], materials science [2], or model bioinorganic chemistry [3]. The phenolic oxygen of salicylaldehyde Schiff base is a potential bridging group to afford high nuclearity complexes. Metal complexes of the well-known tetradentate N_2O_2 salen-type Schiff-base ligands may be bidentate chelating agents (complexes as ligands), coordinating through their *cis*-oxygens to form bi- and tri-nuclear complexes. During the past two decades, linear trinuclear cobalt complexes based on salen-type ligands, such as Co^{II} complexes (Co^{II}–Co^{II}–Co^{II}) [4] and mixed valence cobalt complexes (Co^{III}–Co^{II}–Co^{III}) [5–10], have been widely reported. However, trinuclear cobalt complexes based on tridentate Schiff bases have been rarely reported [11,12]. Moreover, tridentate Schiff bases derived from the monocondensation of salicylaldehyde/substituted salicylaldehyde and aliphatic primary amines, such as diamines [13, 14], amino alcohols [12, 15], and amino acids [16, 17], can bind with one, two, or more

---

*Corresponding author. Email: wangql@nankai.edu.cn

Journal of Coordination Chemistry
ISSN 0095-8972 print/ISSN 1029-0389 online
DOI: 10.1080/00958970903509277

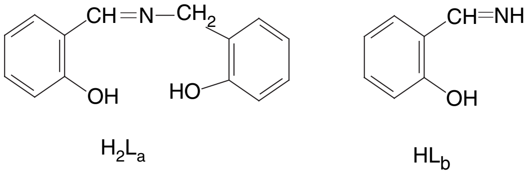

Scheme 1. Structure of the Schiff-base ligands H_2L_a and HL_b.

metal centers involving various coordination modes allowing synthesis of homonuclear metal complexes with interesting stereochemistry. In contrast, salicylaldehyde-derived tridentate Schiff bases of primary amines containing aromatic rings have been much less explored [18–20].

N-(2-hydroxybenzyl)salicylaldimine (H_2L_a) is a tridentate ONO donor Schiff base derived from the reaction of salicylaldehyde and *o*-hydroxybenzylamine, which contains two phenolic oxygen donors (scheme 1). In the diphenoxo-bridged dinuclear Fe^{III} complex $[Fe(L_a)(OAc)]_2$, each L_a^{2-} provides one phenolic oxygen donor as bridging group [21]. In view of the coordination of H_2L_a, we have focused on synthesis, isolation, and characterization of multinuclear complexes of transition metal ions with it and have previously found that it has potential to afford homopolynuclear complexes by facile one-pot reactions [22, 23]. During the course of these investigations, it was observed that upon reacting with $Co(OAc)_2 \cdot 4H_2O$ in dimethylformamide (DMF)–H_2O mixed solvent under air, partial L_a^{2-} underwent the cleavage of C–N single bond to yield salicylaldimine anion (L_b^-) (scheme 1) and a linear mixed-valence trinuclear cobalt complex $[Co^{III}(\mu\text{-}L_a)(\mu\text{-}L_b)(\mu\text{-}OAc)]_2Co^{II} \cdot 2DMF$ (**1**) was formed.

2. Experimental

2.1. *Physical measurements*

Elemental analyses for C, H, and N were carried out on a Perkin-Elmer analyzer (model 240C). IR spectra were recorded as KBr pellets on a Bruker Tensor 27 FTIR spectrophotometer from 400–4000 cm^{-1}. Ultraviolet and visible spectra were measured in DMF solution on a Jasco V-570 UV-Vis/NIR spectrophotometer. Cyclic voltammetry measurements were performed on a BAS Epsilon Electrochemical Workstation. All samples were purged with nitrogen before measurements. Sample solutions (5 mL) were mixed in 10 mL vials. A standard three-electrode system consisting of glassy carbon working electrode, platinum-wire auxiliary electrode, and a saturated calomel electrode (SCE) was used. Variable-temperature magnetic susceptibilities were measured from 2 to 300 K on a Quantum Design MPMS-7 SQUID magnetometer in applied magnetic field of 1000 Oe. Diamagnetic corrections were made with Pascal's constants for all constituent atoms [24].

2.2. *Materials and synthesis*

All solvents and reagents for synthesis were commercially available and used as received. H_2L_a was prepared according to a published procedure [22]. Complex **1** was prepared by adding an aqueous solution (5 mL) of $Co(OAc)_2 \cdot 4H_2O$

Table 1. Crystal data and structure refinement of **1**.

Empirical formula	$C_{26}H_{27}Co_{1.5}N_3O_6$
Formula weight	565.90
Crystal system	Triclinic
Space group	*P-1*
Unit cell dimensions (Å, °)	
a	10.777(2)
b	11.571(2)
c	11.941(2)
α	93.49(3)
β	104.78(3)
γ	114.88(3)
Volume (Å^3), Z	1281.9(4), 2
Calculated density (g cm^{-3})	1.466
μ (mm^{-1})	1.027
$F(000)$	585
λ (Mo-Kα) (Å)	0.71073
Crystal size (mm^3)	0.30 × 0.20 × 0.20
Reflections collected/unique	10721/4504 ($R_{int} = 0.0325$)
Goodness-of-fit on F^2	1.099
Final R indices [$I > 2\sigma(I)$]	$R_1 = 0.0527$, $wR_2 = 0.1135$
R indices, (all data)	$R_1 = 0.0697$, $wR_2 = 0.1210$
Largest difference peak and hole (e Å^{-3})	0.797 and −0.650

(0.1 mmol, 0.0249 g) to a DMF solution (25 mL) of H_2L_a (0.1 mmol, 0.0227 g) under constant stirring. During the 2 h of stirring in air, the color of the reaction mixture changed slowly from red-orange to dark brown. The resulting solution was filtered and the dark brown filtrate was left undisturbed in air at room temperature; well-formed black single crystals of **1** suitable for X-ray structure analysis were obtained by slow evaporation for 6 months. Yield based on $Co(OAc)_2 \cdot 4H_2O$: 27.9 mg, 74%. Anal. Calcd for $C_{26}H_{27}Co_{1.5}N_3O_6$: C, 55.18%; N, 7.42%; H, 4.81%; found C, 55.39%; N, 7.21%; H, 4.59%.

2.3. *Crystal structure determination and refinement*

A crystal of dimensions 0.26 mm × 0.22 mm × 0.20 mm of **1** was mounted on a Bruker Smart 1000 area detector using graphite monochromated Mo-Kα radiation ($\lambda = 0.71073$ Å) at 293(2)K. Structure of **1** was solved by direct methods and successive Fourier difference syntheses (SHELXS-97) [25] and refined by full-matrix least-squares on F^2 with anisotropic thermal parameters for all non-hydrogen atoms (SHELXL-97) [26]. Crystal data and details of refinement are summarized in table 1. Selected bond distances and angles are given in table 2.

3. Results and discussion

3.1. *Synthesis*

Complex **1** $[Co^{III}(\mu\text{-}L_a)(\mu\text{-}L_b)(\mu\text{-}OAc)]_2Co^{II} \cdot 2DMF$, was synthesized by reaction of $Co(OAc)_2 \cdot 4H_2O$ with H_2L_a in DMF-H_2O. Atmospheric oxygen acts as an external oxidant [5, 8, 10]. The aerial oxidation of the Co^{II} precursor may be facilitated because

Table 2. Selected bond distances (Å) and angles (°) of **1**.

Bond	Distance (Å)	Bond	Distance (Å)
Co(1)–N(3)	1.876(3)	Co(2)–O(5)	2.027(2)
Co(1)–O(1)	1.876(3)	Co(2)–O(2)	2.093(2)
Co(1)–N(1)	1.900(3)	Co(2)–O(3)	2.132(2)
Co(1)–O(3)	1.917(2)	C(7)–N(1)	1.280(5)
Co(1)–O(2)	1.921(3)	C(8)–N(1)	1.464(5)
Co(1)–O(6)	1.954(3)	C(26)–O(7)	1.039(11)
		C(21)–N(3)	1.271(5)
Bond	Angle (°)	Bond	Angle (°)
N(3)–Co(1)–O(1)	90.02(14)	O(5)–Co(2)–O(5A)	180.000(1)
N(3)–Co(1)–N(1)	88.89(15)	O(5)–Co(2)–O(2)	86.70(10)
O(1)–Co(1)–N(1)	94.09(14)	O(5A)–Co(2)–O(2)	93.30(10)
N(3)–Co(1)–O(3)	92.91(13)	O(5)–Co(2)–O(2A)	93.30(10)
O(1)–Co(1)–O(3)	88.22(12)	O(5A)–Co(2)–O(2A)	86.70(10)
N(1)–Co(1)–O(3)	177.07(13)	O(2)–Co(2)–O(2A)	180.0
N(3)–Co(1)–O(2)	92.56(13)	O(5)–Co(2)–O(3)	88.67(10)
O(1)–Co(1)–O(2)	172.46(10)	O(5A)–Co(2)–O(3)	91.33(10)
N(1)–Co(1)–O(2)	93.04(13)	O(2)–Co(2)–O(3)	75.35(10)
O(3)–Co(1)–O(2)	84.58(11)	O(2A)–Co(2)–O(3)	104.65(10)
N(3)–Co(1)–O(6)	174.86(13)	O(5)–Co(2)–O(3A)	91.33(10)
O(1)–Co(1)–O(6)	88.43(12)	O(5A)–Co(2)–O(3A)	88.67(10)
N(1)–Co(1)–O(6)	86.33(12)	O(2)–Co(2)–O(3A)	104.65(10)
O(3)–Co(1)–O(6)	91.95(10)	O(2A)–Co(2)–O(3A)	75.35(10)
O(2)–Co(1)–O(6)	89.59(11)	O(3)–Co(2)–O(3A)	180.000(1)
Co(1)–O(2)–Co(2)	98.32(11)	Co(1)–O(3)–Co(2)	97.11(11)

H_2L_a and its substituted derivatives can stabilize some transition metal ions of higher oxidation states, such as Co^{III} [27] and Mn^{IV} [28, 29]. At the same time coordination of Co^{III} with L_a^{2-} may play an important role for C–N single bond cleavage of L_a^{2-} and *in situ* ligand transformation. The Ru^{II} [30, 31] and Mn^{III} [32] mediated C–N single bond cleavage resulting in Schiff-base ligand transformation during complex formation have been reported. However, Co^{II}- or Co^{III}-mediated C–N single bond cleavage has rarely been reported. In addition, **1** is the first homopolynuclear cobalt complex based on H_2L_a or HL_b.

3.2. *Crystal structure*

The structure of **1** consists of neutral trinuclear $Co_3(L_a)_2(L_b)_2(OAc)_2$ units and DMF. A perspective view of the trinuclear unit is shown in figure 1. Co(2) lies on a center of symmetry and Co(1) is in a general position. L_a^{2-} is terminally bonded to Co(1) through both phenolate oxygens (O(1) and O(2)) and the imine nitrogen (N(1)). O(2) arising from *o*-hydroxybenzylamine forms a bridge between Co(1) and Co(2). L_b^{-} coordinates bidentate to Co(1) and also acts as a bridging ligand between Co(1) and Co(2) utilizing its phenolate oxygen O(3). The OAc^- anion utilizes both its carboxylate atoms (O(5) and O(6)) to form a μ_2-O,O′ bridge. Adjacent Co $\cdots$ Co intramolecular separations are 3.039 Å, not sufficiently short to afford metal–metal bonding or allow intra-metal spin exchange through mutual interaction.

The coordination environments of the two independent cobalt atoms are different. The central Co(2) has a CoO_6 tetragonally distorted octahedral geometry, with the unique axial Co(2)–O(5) bond distance (2.027 Å) being a little shorter than the

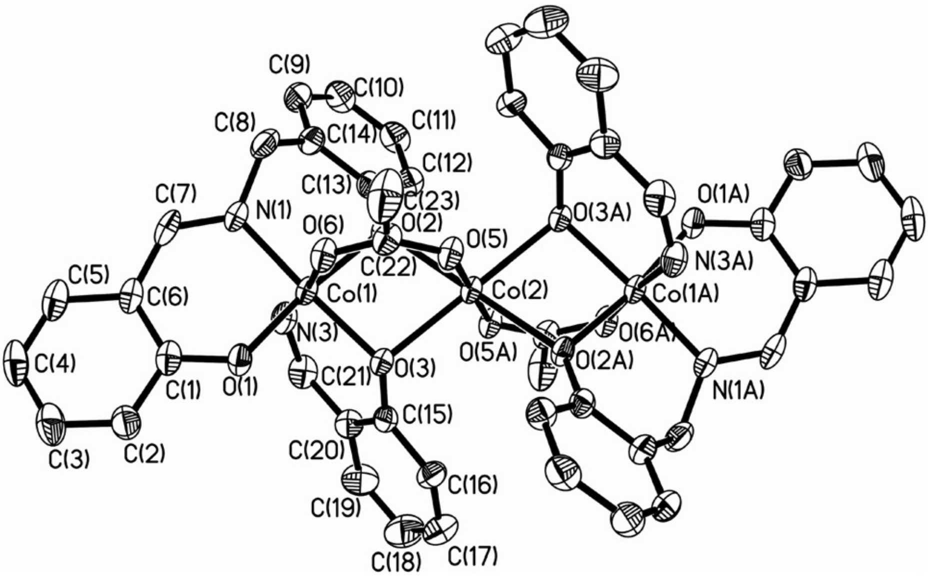

Figure 1. Structure of $[Co^{III}(\mu\text{-}L_a)(\mu\text{-}L_b)(\mu\text{-}OAc)]_2Co^{II}$; hydrogen atoms are omitted for clarity.

equatorial Co(2)–O(2) and Co(2)–O(3) bond distances (2.093 and 2.132 Å, respectively). The terminal atom Co(1) shows a CoN_2O_4 pseudo-octahedral geometry, in which two phenolate oxygens (O(1) and O(2)), one imine nitrogen (N(1)) from L_a^{2-} and one phenolate oxygen (O(3)) from L_b^- define the equatorial plane and the two apical positions are coordinated by imine nitrogen (N(3)) from L_b^- and acetate oxygen (O(6)). The bond distances around Co(1) (Co(1)–O = 1.876–1.954 and Co(1)–N = 1.876–1.900 Å) are significantly shorter than those around Co(2), suggesting that the oxidation states of these cobalt atoms are different. Charge considerations require a formal Co_2^{III} Co^{II} description of **1**, and thus we can assign the Co(1) and Co(1A) atoms to low-spin Co^{III} and the Co(2) atom to high-spin Co^{II}, based on the coordination geometries and bonding parameters [7, 33]. All the Co^{III}–O, Co^{III}–N, and Co^{II}–O distances observed in **1** agree well with the corresponding bond distances observed in linear mixed-valence trinuclear cobalt complexes based on the salen-type ligands [5–10]. All the Co–O bond distances lengthen as follows: $Co^{III}\text{–}O(L_a^{2-})_{phen} < Co^{III}\text{–}O(L_b^-)_{\mu\text{-phen}} < Co^{III}\text{–}O(L_a^{2-})_{\mu\text{-phen}} < Co^{III}\text{–}O_{\mu\text{-acetate}} < Co^{II}\text{–}O_{\mu\text{-acetate}} < Co^{II}\text{–}O(L_a^{2-})_{\mu\text{-phen}} < Co^{II}\text{–}O(L_b^-)_{\mu\text{-phen}}$. The bond distances of C(21)–N(3) and C(7)–N(1) are 1.271 and 1.280 Å, respectively, which are normal for C=N [30].

Figure 2 shows the packing diagram of **1**. The separation of O(7) ⋯ N(3) is 2.842 Å, suggesting the presence of an intermolecular H-bond between the $Co_3(L_a)_2(L_b)_2(OAc)_2$ unit and the neighboring DMF molecule. The crystals are packed via van der Waals contacts between discrete units and the N–H ⋯ O intermolecular H-bonds, with the neighboring $Co^{II} \cdots Co^{II}$ separations between 10.777 and 13.895 Å.

3.3. *Spectroscopic properties*

IR spectra of **1** exhibit a broad, strong band centered at 3400 cm^{-1}, attributed to the N–H stretch of L_b^- [30, 34]. The C=O stretch at 1664 cm^{-1} is shifted to lower frequency

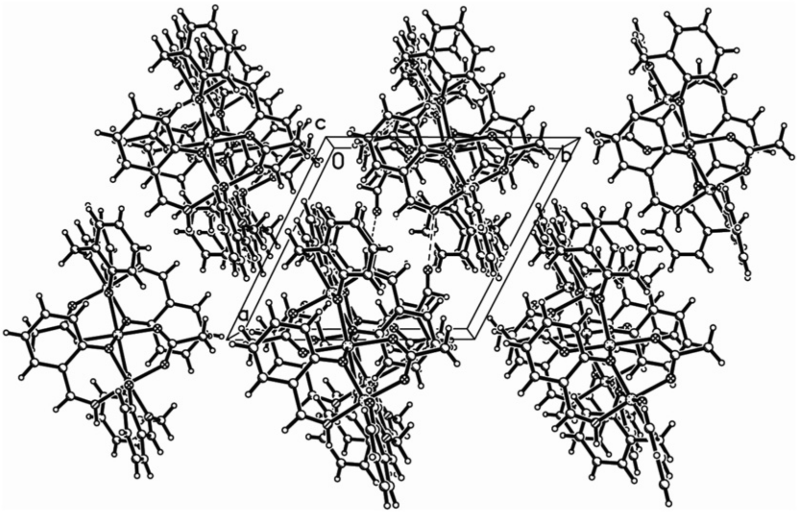

Figure 2. Packing diagram of **1**.

by 14 cm^{-1} with respect to the standard IR spectrum of DMF film, owing to formation of an intermolecular H-bond [35,36]. Another intense band at 1635 cm^{-1} and medium band at 1595 cm^{-1} may be assigned to C=N stretch of the conjugated imine of L_a^{2-} and L_b^-, respectively [22, 30, 37]. The red shift of the C=N absorption of 24 cm^{-1} on going from free H_2L_a to **1** suggests weak π-accepting ability of the coordinated ligands. Vibrationally active acetate ligands display antisymmetric and symmetric stretching vibrations at 1574 and 1409 cm^{-1}, respectively. The difference in frequency $\Delta(\nu_{asm}(COO^-) - \nu_{sym}(COO^-))$ is 165 cm^{-1} (163 cm^{-1} for free acetate ion), indicating the presence of deprotonated carboxylate coordinated to metal centers in a bridged bidentate fashion [5, 8]. The C–O stretch at 1303–1349cm^{-1} indicates that the phenolic oxygen of L_a^{2-} and L_b^- are bonded to cobalt [7, 38].

The electronic spectrum of **1** in DMF was recorded in the range 190–800 nm (λ_{max} (ϵ, L mol^{-1} cm^{-1}) 272 (65,700), 374 (15,200), 550 (920), 650 (383)nm). The ultraviolet absorption bands observed for **1** at 272 and 374 nm are more intense than the visible bands, and the tail into the visible region accounts for the black appearance of **1**. The absorption band at 272 nm may be assigned to π–π* intraligand transitions in the benzene ring and azomethine groups. The absorption at 374 nm may be assigned to ligand to metal charge transfer (LMCT). Two very weak absorptions in the visible range at 550 and 650 nm are tentatively attributed to the Laporte Forbidden d–d transitions of Co^{III} and Co^{II} in octahedral geometry [8,10,39].

3.4. *Electrochemistry*

Cyclic voltammetry was performed within the potential range −2.0 to +2.0 V under different scan rates (0.02–1.0 V s^{-1}) at ambient temperature (300 K). In DMF (1.0×10^{-3} mol L^{-1}), **1** displayed a quasi-reversible reductive response at −1.46 V (Supplementary material) with characteristic anodic (E_{pa}) and cathodic (E_{pc}) peak

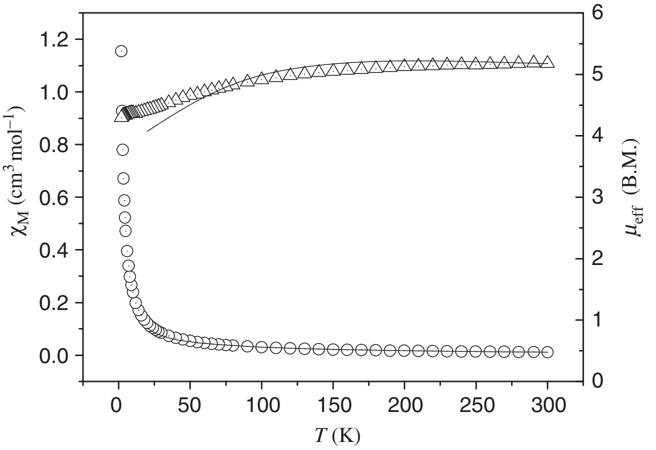

Figure 3. χ_M(O) and μ_{eff}(Δ) *vs.* temperature curves for **1**. The solid lines represent the theoretical values based on equation (3).

potentials at −1.40 and −1.52 V, respectively. The quasi-reversible signal is attributed to $Co^{III} \rightarrow Co^{II}$ reduction. The relevant electron transfer is represented in equation (1).

$$[Co^{III}-Co^{II}-Co^{III}] + 2e \rightarrow [Co^{II}-Co^{II}-Co^{II}]^{2-}. \tag{1}$$

The oxidation reaction was commenced at *ca.* +0.99 V in the anode sweep whereas no response at the counter cathode sweep was observed. The irreversible response is assigned to the $Co^{II} \rightarrow Co^{III}$ oxidation (equation (2)).

$$[Co^{III}-Co^{II}-Co^{III}] \rightarrow [Co^{III}-Co^{III}-Co^{III}]^{+} + e. \tag{2}$$

However, in acetonitrile solution (1.0×10^{-3} mol L^{-1}) **1** displayed irreversible reductive and oxidative response at *ca* −1.10 and +1.00 V, respectively, indicating that reduction of Co^{III} is easier in acetonitrile than in DMF.

3.5. *Magnetic properties*

As shown in figure 3, the value of μ_{eff} (where μ_{eff} is the effective magnetic moment) of **1** at room temperature is 5.18 μ_B, larger than the spin-only value (3.87μ_B) for $S = 3/2$ with $g = 2.0$, but agreeing with values observed for octahedral Co^{II} complexes with a significant first-order orbital contribution to the magnetic moment, typical of the $^4T_{1g}$ ground state [33, 40, 41]. The μ_{eff} plot gradually decreases with decreasing temperature and reaches a minimum value of 4.30 μ_B at 2 K, therefore Co^{II} remains totally in the high-spin state down to 2 K and we expect an important orbital contribution in all cases. These magnetic data confirm that **1** is in the mixed valence state $Co^{III}(S=0)$–$Co^{II}(S=3/2)$–$Co^{III}(S=0)$ as suggested by the X-ray structural analysis. The decrease of μ_{eff} with decreasing temperature may be mainly due to depopulation of the higher energy Kramers doublets of the Co^{II} centers [42].

In order to interpret the magnetic properties of **1**, the contributions of spin–orbit coupling and Zeeman interaction to spin-only value should be taken into consideration. Here, we tried to analyze the experimental data using the one-ion approximation for

Co^{II} with spin–orbit coupling in O_h symmetry. As the neighboring $Co^{II} \cdots Co^{II}$ separations are long, the exchange coupling between the Co^{II} centers is expected to be very weak and neglectable. The resulting magnetic susceptibility equation is shown in equation (3), where λ is the spin–orbit coupling constant.

$$\begin{aligned}
\chi_{\mathrm{Co}} &= \frac{N\beta^2}{3KT}\left[\frac{N}{D}\right] \\
N &= \frac{7(3-A)^2x}{5} + \frac{12(A+2)^2}{25A} + \left\{\frac{2(11-2A)^2x}{45} + \frac{176(A+2)^2}{675A}\right\}\exp\left(\frac{-5Ax}{2}\right) \\
&\quad + \left\{\frac{(A+5)^2x}{9} - \frac{20(A+2)^2}{27A}\right\}\exp(-4Ax) \qquad (3) \\
D &= \frac{x}{3}\left[3 + 2\exp\left(\frac{-5Ax}{2}\right) + \exp(-4Ax)\right] \\
A &= 1.5, \quad x = \frac{\lambda}{kT}.
\end{aligned}$$

The parameters N and β have their usual meanings. The value of A ranges from 1.5 to 1 when the crystal field changes from the weak limit to the strong limit. As for most magnetic studies of Co^{II}, here we give $A = 1.5$ for octahedral Co^{II} surrounded by six oxygen atoms. The best fit parameter of the experimental data in the temperature range 20–300 K is $\lambda = -121\,\mathrm{cm}^{-1}$ with agreement factor 1.30×10^{-3} ($R = \sum(\chi_{\mathrm{obsd}} - \chi_{\mathrm{calcd}})^2 / \sum \chi_{\mathrm{obsd}}^2$). The value of λ is smaller than that of the free ion ($\lambda_0 = -176\,\mathrm{cm}^{-1}$) due to covalency effects, which is close to that of the high-spin $Co^{II}O_6$ complex ($\lambda = -133\,\mathrm{cm}^{-1}$) [43].

4. Conclusions

Combination of the tridentate ONO donor Schiff-base H_2L_a and $Co(OAc)_2 \cdot 4H_2O$ afforded a unique Co^{III}–Co^{II}–Co^{III} linear trinuclear complex **1** via an *in situ* ligand transformation based on C–N bond cleavage of H_2L_a and partial oxidation of the Co^{II} precursor. To the best of our knowledge, **1** is the first homopolynuclear cobalt complex based on H_2L_a or HL_b. Complex **1** is reduced quasi-reversibly at −1.46 V and oxidized irreversibly at *ca.* +0.99 V by cyclic voltammetry at room temperature in DMF. Cryomagnetic investigations in the range 2–300 K confirm that **1** is in the mixed valence state $Co^{III}(S=0)$–$Co^{II}(S=3/2)$–$Co^{III}(S=0)$ and reveal the contributions of spin–orbit coupling to magnetic susceptibility with $\lambda = -121\,\mathrm{cm}^{-1}$.

Supplementary material

Crystallographic data for the structural analysis have been deposited with the Cambridge Crystallographic Data Centre as supplementary publication No. CCDC 723458. Copies of the data can be obtained free of charge from the Director, CCDC, 12 Union Road, Cambridge CB2 1EZ, UK (Fax: +44-1223-336-033; E-mail: deposit@ccdc.cam.ac.uk). Fig. S1. Cyclic voltammogram of complex **1**.

Acknowledgements

This work was supported by the National Natural Science Foundation of China (No. 20601014), the National Basic Research Program of China (973 Program, 2007CB815305) and the Natural Science Research Program of the Education Department of Hebei Province (No. Z2008107).

References

[1] (a) O. Kahn, J. Larionova, J.V. Yakhmi. *Chem. Eur. J.*, **5**, 3443 (1999); (b) D.J. Price, S.R. Batten, B. Moubaraki, K.S. Murray. *Chem. Commun.*, 762 (2002); (c) R. Sessoli, H.L. Tsai, A.R. Schake, S. Wang, J.B. Vincent, K. Folting, D. Gatteschi, G. Christou, D.N. Hendrickson. *J. Am. Chem. Soc.*, **115**, 1804 (1993); (d) J.S. Miller. *Inorg. Chem.*, **39**, 4392 (2000); (e) T. Glaser, M. Heidemeier, E. Krickemeyer, H. Bögge, A. Stammler, R. Fröhlich, E. Bill, J. Schnack. *Inorg. Chem.*, **48**, 607 (2009).

[2] (a) K. Biradha, Y. Hongo, M. Fujita. *Angew. Chem. Int. Ed.*, **39**, 3843 (2000); (b) K. Seki, S. Takamizawa, W. Mori. *Chem. Lett.*, 332 (2001).

[3] (a) J. Hong, O.A. Kharenko, M.Y. Ogawa. *Inorg. Chem.*, **45**, 9974 (2006); (b) M.A. Halcrow, G. Christou. *Chem. Rev.*, **94**, 2421 (1994); (c) N. Raman, S. Johnson Raja, A. Sakthivel. *J. Coord. Chem.*, **62**, 691 (2009); (d) R.M. Issa, S.A. Azim, A.M. Khedr, D.F. Draz. *J. Coord. Chem.*, **62**, 1859 (2009); (e) W. Luo, X.G. Meng, G.Z. Cheng, Z.P. Ji. *J. Coord. Chem.*, **62**, 1492 (2009).

[4] (a) D.H. Shi, Z.L. You, C. Xu, Q. Zhang, H.L. Zhu. *Inorg. Chem. Commun.*, **10**, 404 (2007); (b) Z.L. You, P. Zhou. *Inorg. Chem. Commun.*, **10**, 1273 (2007); (c) A. Gerli, K.S. Hagen, L.G. Marzilli. *Inorg. Chem.*, **30**, 4673 (1991).

[5] S. Banerjee, J.T. Chen, C.Z. Lu. *Polyhedron*, **26**, 686 (2007).

[6] X. He, C.Z. Lu, C.D. Wu. *J. Coord. Chem.*, **59**, 977 (2006).

[7] J. Welby, L.N. Rusere, J.M. Tanski, L.A. Tyler. *Inorg. Chim. Acta*, **362**, 1405 (2009).

[8] S. Chattopadhyay, G. Bocelli, A. Musatti, A. Ghosh. *Inorg. Chem. Commun.*, **9**, 1053 (2006).

[9] C. Fukuhara, E. Asato, T. Shimoji, K. Katsura, M. Mori, K. Matsumoto, S. Ooi. *J. Chem. Soc., Dalton Trans.*, 1305 (1987).

[10] S. Chattopadhyay, M.G.B. Drew, A. Ghosh. *Eur. J. Inorg. Chem.*, 1693 (2008).

[11] H.L. Zhu, X.Y. Liu. *Synth. React. Inorg., Met.–Org., Nano–Met. Chem.*, **35**, 193 (2005).

[12] C.P. Pradeep, P.S. Zacharias, S.K. Das. *Eur. J. Inorg. Chem.*, 5377 (2007).

[13] S. Banerjee, M.G.B. Drew, C.Z. Lu, J. Tercero, C. Diaz, A. Ghosh. *Eur. J. Inorg. Chem.*, 2376 (2005).

[14] H.D. Bian, W. Gu, J.Y. Xu, F. Bian, S.P. Yan, D.Z. Liao, Z.H. Jiang, P. Cheng. *Inorg. Chem.*, **42**, 4265 (2003).

[15] H.Y. Liu, H.Y. Wang, D.Z. Niu, Z.S. Lu, J. Sun. *Synth. React. Inorg., Met.–Org., Nano–Met. Chem.*, **35**, 233 (2005).

[16] R. Karmakar, C.R. Choudhury, S. Mitra, L. Dahlenburg. *Struct. Chem.*, **16**, 611 (2005).

[17] P.A.N. Reddy, M. Nethaji, A.R. Chakravarty. *Eur. J. Inorg. Chem.*, 1440 (2004).

[18] H.Y. Liu, F. Gao, D.Z. Niu, J.L. Tian. *Inorg. Chim. Acta*, **362**, 4179 (2009).

[19] O. Pouralimardan, A.C. Chamayou, C. Janiak, H. Hosseini-Monfared. *Inorg. Chim. Acta*, **360**, 1599 (2007).

[20] A.D. Garnovskii, I.S. Vasilchenko, D.A. Garnovskii, B.I. Kharisov. *J. Coord. Chem.*, **62**, 151 (2009).

[21] M. Mikuriya, Y. Kakuta, R. Nukada, T. Kotera, T. Tokii. *Bull. Chem. Soc. Japan*, **74**, 1425 (2001).

[22] Q.L. Wang, C. Yang, L. Qi, D.Z. Liao, G.M. Yang, H.X. Ren. *J. Mol. Struct.*, **892**, 88 (2008).

[23] C. Yang, Q.L. Wang, G.T. Tang, P. Sun, G.F. Xu, D.Z. Liao. *Chinese J. Struct. Chem.*, **28**, 636 (2009).

[24] P.W. Selwood. *Magnetochemistry*, 2nd Edn, p. 78, Wiley-Interscience, New York (1956).

[25] G.M. Sheldrick. *SHELXS-97, Program for Solution of Crystal Structures*, University of Göttingen, Göttingen, Germany (1997).

[26] G.M. Sheldrick. *SHELXL-97, Program for the Refinement of Crystal Structures*, University of Göttingen, Göttingen, Germany (1997).

[27] K. Jitsukawa, T. Hata, T. Yamamoto, K. Kano, H. Masuda, H. Einaga. *Chem. Lett.*, **7**, 1169 (1994).

[28] M. Mikuriya, S. Shigematsu, K. Kawano, T. Tokii, H. Oshio. *Chem. Lett.*, **12**, 729 (1990).

[29] M. Mikuriya, D. Jie, Y. Kakuta, T. Tokii. *Bull. Chem. Soc. Japan*, **66**, 1132 (1993).

[30] S. Chakraborty, M.G. Walawalkar, G.K. Lahiri. *J. Chem. Soc., Dalton Trans.*, 2875 (2000).

[31] S. Chakraborty, M.G. Walawalkar, G.K. Lahiri. *Polyhedron*, **20**, 1851 (2001).

[32] M. Maneiro, M.R. Bermejo, M.I. Fernández, A.M. González-Noya, A.M. Tyryshkin, R.G. Pritchard. *Z. Anorg. Allg. Chem.*, **629**, 285 (2003).

[33] B. Żurowska, A. Brzuszkiewicz. *Polyhedron*, **27**, 1623 (2008).
[34] B.B. Koleva, Ts. Kolev, M. Spiteller. *Inorg. Chim. Acta*, **360**, 2224 (2007).
[35] L.S. Wang, T.L. Sheng, J.J. Zhang, S.M. Hu, R.B. Fu, X.T. Wu, Y.M. Li, X.H. Huang, S.C. Xiang. *Polyhedron*, **26**, 1098 (2007).
[36] H.R. Wen, C.F. Wang, Y. Song, S. Gao, J.L. Zuo, X.Z. You. *Inorg. Chem.*, **45**, 8942 (2006).
[37] X. Chen, F.J. Femia, J.W. Babich, J. Zubieta. *Inorg. Chim. Acta*, **306**, 113 (2000).
[38] T. Glaser, M. Gerenkamp, R. Fröhlich. *Angew. Chem. Int. Ed.*, **41**, 3823 (2002).
[39] D.A. Knight, J.R. Deschamps, R.J. Butcher, C. Simmers, E.L. Chang. *Polyhedron*, **27**, 1795 (2008).
[40] F. Dumestre, B. Soula, A.M. Galibert, P.L. Fabre, G. Bernardinelli, B. Donnadieu, P. Castan. *J. Chem. Soc., Dalton Trans.*, 4131 (1998).
[41] R. March, W. Clegg, R.A. Coxall, L. Cucurull-Sánchez, L. Lezama, T. Rojo, P. González-Duarte. *Inorg. Chim. Acta*, **353**, 129 (2003).
[42] J.M. Herrera, A. Bleuzen, Y. Dromzée, M. Julve, F. Lloret, M. Verdaguer. *Inorg. Chem.*, **42**, 7052 (2003).
[43] L. Cañadillas-Delgado, O. Fabelo, J. Pasán, F.S. Delgado, F. Lloret, M. Julve, C. Ruiz-Pérez. *Inorg. Chem.*, **46**, 7458 (2007).